Modeling the Influence of Grains and Material Interfaces on Electromigration

Lado Filipovic
Institute for Microelectronics, TU Wien
1040 Wien, Austria
filipovic@iue.tuwien.ac.at

Roberto Lacerda de Orio
School of Electrical and Computer Engineering, UNICAMP
13083-852 Campinas-SP, Brazil
orio@fee.unicamp.br

***Abstract*—We present an efficient approach to properly treat grain boundaries and material interfaces when modeling electromigration in copper nano-interconnects. Our approach uses several spatial material parameters to identify the locations of the grain boundaries and material interfaces during simulation, thereby not requiring the definition of multiple materials or complex meshes and geometrical interfaces. Using this method even very coarse meshes, with a grid spacing twice the size of the thinnest element (the grain boundary thickness), were able to reasonably reproduce the vacancy concentration of thin copper interconnects, including the microstructure. However, using a grid spacing greater than one half the grain boundary thickness resulted in underestimates of the induced stress.**

***Index Terms*—Electromigration, Modeling and simulation, TCAD, Nano-interconnects, Copper, Back-end-of-line**

I. Introduction

The continued trend in transistor scaling is being bolstered by a simultaneous scaling in metal interconnects. However, the consistent shrinking of metal lines gives rise to several undesired effects, including an increased resistivity and current density, potentially resulting in a reduced interconnect lifetime. When the thickness of a copper line is reduced, the average crystal grain size decreases almost linearly, as characterized by Sun et al. [1]. This decrease in grain size and the overall reduction in the metal thickness means that grain boundaries (GBs) and material interfaces (MIs) play an increasingly important role in the conductive behavior of metals. The influence of GB and MI electron scattering has been explored most notably by Mayadas and Schatzkes [2] as well as Fuchs [3] and Sondheimer [4].

Along with the changes in the conductive behavior of copper nano-interconnects, the reliability of the metal lines is also significantly influenced by the granular microstructure. Electromigration (EM) is the major reliability concern in the metal interconnects, present in modern integrated circuits. EM degradation results in chip failure due to the nucleation and subsequent growth of a void, which ultimately leads to an increasing line resistance and an open circuit failure [5]. Many attempts are underway to replace metallic interconnects with EM-resistant alternatives, such as carbon nanotubes [6], [7]. However, due to the planned continued use of copper nano-interconnects for advanced nodes up to 7nm [8], we need to make sure that EM is properly modeled and that nano-interconnect lifetimes can be appropriately estimated.

II. Electromigration

Current state-of-the-art models for EM struggle to appropriately simulate the complex copper microstructure, where GBs and MIs perform several important functions. In addition to their influence on the copper conductivity, they serve as fast vacancy diffusion pathways and vacancy generation and annihilation sites [9]. Recently an attempt was made to model EM with microstructure by including GBs and MIs as spatial parameters using the distance from a GB or MI as a material parameter [10]. This distance parameter was then used to determine the electrical conductivity σ of the copper line as well as the essential variables of the vacancy diffusion coefficient given by

$$D_v = D_{v0} \exp\left(\frac{E_a}{k_B T}\right), \tag{1}$$

where k_B is the Boltzmann constant and T is the temperature. The pre-exponential factor for vacancy diffusion D_{v0} and the activation energy for diffusion E_a vary between the crystalline grain, GB, and MI according to Table I [5], [9]. The main drawback in the method presented previously in [10] is that the GB and MI were not differentiated and were treated as a single scatter event (SE) with a single set of material parameters. The values of E_a=0.7eV and D_{v0}=52cm^2/s were used for both GBs and MIs, leading to potential errors in the simulations. This has been updated in the model presented in this manuscript, where the MI and GB are treated fully independently.

TABLE I
Microstructure-dependent material parameters for the vacancy dynamics model from [5], [9].

Vacancy diffusion parameter	Grain	GB	MI
Activation energy (E_a) eV	0.89	0.7	0.5
Pre-exponential factor (D_{v0}) cm^2/s	0.52	52	520

In addition, the method presented previously diminishes the effective influence of the MI in the model since the E_a and D_{v0} values inside GBs and MIs were assigned according to the distance from a SE being less than one half of the effective boundary thickness. The GB is characterized as the distance from the GB in both directions, while the MI only has one relevant direction, resulting in its effective thickness being one half that of the GB thickness.

978-1-5386-6790-3/18/$31.00 ©2018 IEEE

III. Electromigration Modeling Framework

In the modeling framework described here the grain bulk, grain boundaries, and material interfaces are differentiated using spatial material parameters instead of defining different materials, which potentially requires complex meshes. There are three key steps to the framework, as visualized in Fig. 1:

1) Grain tessellation: The open-source software Neper [11] is used to generate the crystalline copper geometry.
2) The microstructured geometry is imported into an in-house tool, where a Cartesian grid is generated. Each point on the grid is assigned several parameter values, including distance to the nearest SE and atom diffusivity.
3) The spatial parameters are then imported into a finite element simulator, where the EM model is implemented and simulations are run. In this study, COMSOL Multi-physics [12] was used for the EM simulations.

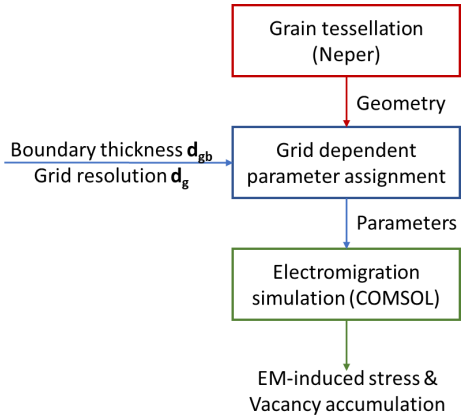

Fig. 1. Three phases of the implemented modeling framework to properly simulate electromigration in copper nano-interconnects, while taking grain boundaries and material interfaces into consideration.

A. Grain Tessellation

In this work, we test our model using a sample two-dimensional (2D) interconnect line with dimensions 20nm×2000nm and an average grain size of 25nm, which fits with grain sizes measured in [1]. This results in a columnar grain structure, with a few sections where grains appear stacked on top of each other, as depicted in Fig. 2. From the top to the bottom of Fig. 2 we show the left, middle, and right sections of the granular copper geometry. This geometry is then imported into an in-house tool in order for the appropriate spatial material parameters to be assigned and overlayed on top of the generated microstructure.

B. Spatial Parameter Assignment

The spatial parameters which identify the location of the GB and MI are explicitly defined on all Cartesian mesh intersect points, while a linear interpolation is used to populate the entire material domain. This proceeds according to the flowchart shown in Fig. 3. First, the microstructure is imported and a desired boundary thickness and grid resolution are assigned. GB and MI thicknesses of 1nm were assumed for most of this study, because this value was found to be appropriate from

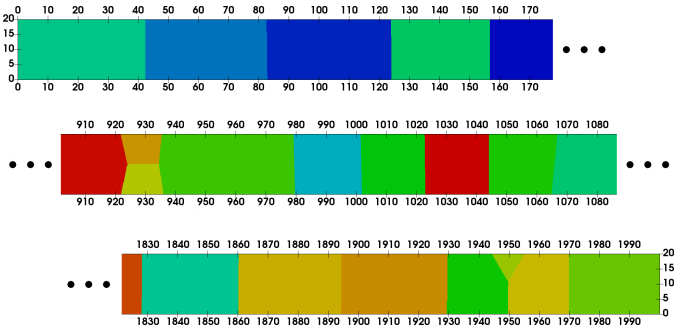

Fig. 2. Granular structure for the copper line used in this study with axes in [nm]. (top) Left-most section of the line, with the columnar structure evident. (middle) Middle section where one sample of a stacked grain is evident. (bottom) Right-most section with more complex features.

previous publications [13]. According to this, all grid points are iterated and material parameters are assigned for each grid point according to Fig. 3 as follows:

- Iterate through the grains until the grain in which the current point is located is identified.
- Find the nearest edge for the given grid point. An edge can be a grain boundary or a material interface.
- Find the distance from the nearest edge. This distance is one of the key parameters for the material conductivity.
- If the distance to the nearest edge is greater than the defined boundary thickness, bulk parameters for D_{v0} and E_a are assigned to that point.
- If the distance to the nearest edge is smaller than the defined boundary thickness, then the GB or MI parameters for D_{v0} and E_a are assigned, depending on whether the nearest edge is a GB or a MI, respectively.

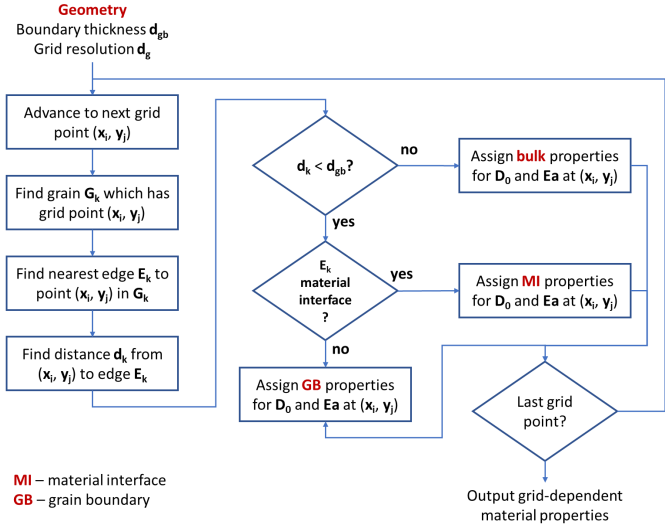

Fig. 3. Flow chart for the process of assigning the necessary material parameters to each grid point in the simulation space.

The results of the process from Fig. 3 are shown in Fig. 4. In Fig. 4 (top), the distance to the nearest edge is plotted. This value is used to calculate the local conductivities inside the thin film. Fig. 4 (middle) and Fig. 4 (bottom) depict the assignment of the grid points for the pre-exponential factor D_{v0} and activation energy E_a from (1) as given in Table I.

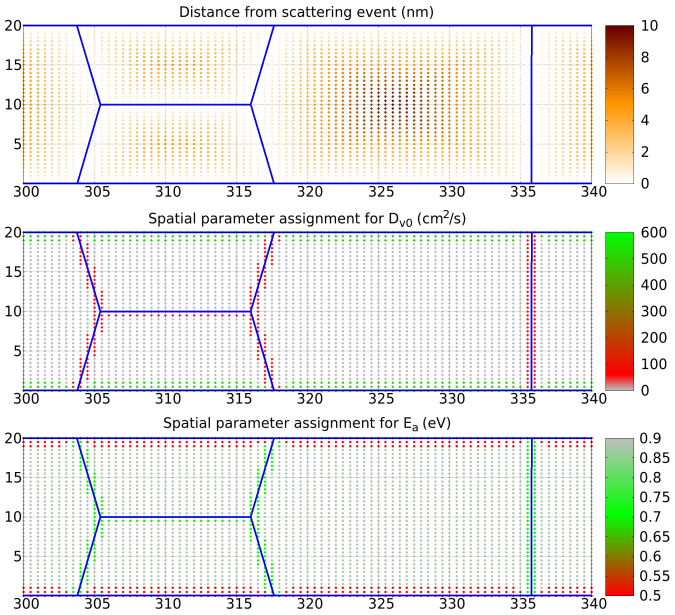

Fig. 4. Spatial parameters used in this study in order to properly treat the GB and MI. The grid size shown in all figures above is 0.5nm.

C. Electromigration Model

The EM model requires the simultaneous solution of three physical models including calculating the temperature and current density for the electro-thermal problem, vacancy dynamics, and solid mechanics. Ultimately, the EM-induced stress, as shown in Fig. 5, is found.

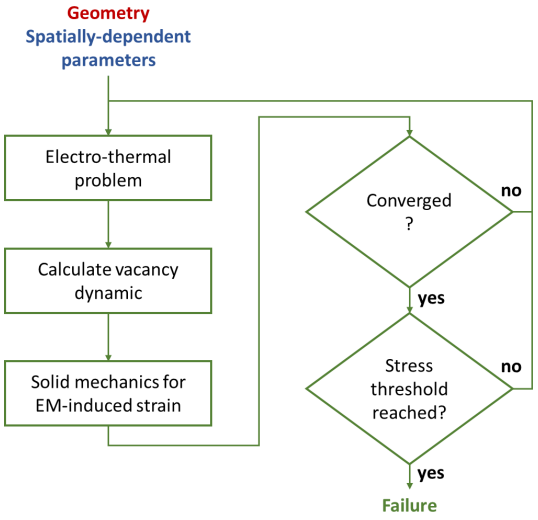

Fig. 5. Flow chart for the electromigration model.

1) Copper resistivity: By applying the microstructure-dependent resistivity given by Clarke et al. [14], an expression for the resistivity with respect to the distance to the nearest scattering event λ_s has been derived

$$\rho = \rho_b \left(1 + \frac{3 \cdot \lambda}{8 \cdot \lambda_s}\right), \tag{2}$$

with ρ_b the bulk resistivity and λ the electron mean free path (MFP). When we treat the GB and MI as 1nm thick layers, a MFP of 4nm, and a bulk resistivity of $1.68 \times 10^{-8} \Omega \cdot$m, we obtain the resistivity measured in by Sun et al. [1]. The distance from a scattering even and the resulting conductivity through the copper is microstructure dependent, as depicted in Fig. 6 top and bottom, respectively.

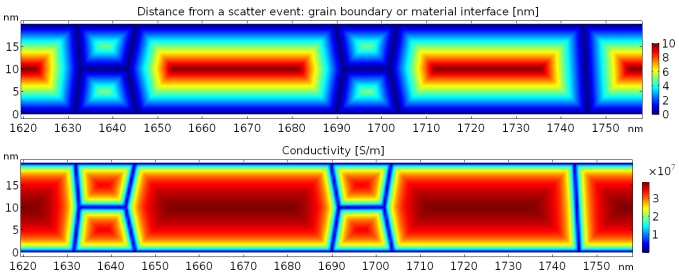

Fig. 6. Spatial parameters implemented within the finite element tool with: (top) The distance from a GB or MI and (bottom) The resulting spatial microstructure-dependent conductivity within the thin copper line.

2) Electromigration Model: The TCAD model used to calculate the vacancy dynamics and EM-induced stress is given in [9]. The total vacancy flux is given by

$$\vec{J_v} = -D_v \left[\nabla C_v + C_v \left(\frac{eZ^*}{kT}\rho\vec{j} - \frac{Q^*}{kT^2}\nabla T + \frac{f\Omega}{kT}\nabla\sigma\right)\right], \tag{3}$$

with C_v the vacancy concentration, e the elementary charge, Z^* the effective charge, $\vec{j}$ the current density, Q^* the heat of transport, f the vacancy relaxation ration, Ω the atomic volume, and σ the hydrostatic stress. The accumulation and depletion of vacancies is found according to the continuity equation

$$\frac{\partial C_v}{\partial t} = -\nabla \cdot \vec{J_v} + G, \tag{4}$$

where G is a surface function which models vacancy generation and annihilation, taking place at GBs and MIs only. This term is applied using

$$G = \frac{\partial C_{v,T}}{\partial t} = \frac{\chi}{\tau}\left[C_{v,eq} - C_{v,T}\left(1 + \frac{\omega_R}{\omega_T C_v}\right)\right], \tag{5}$$

where $C_{v,T}$ and $C_{v,eq}$ are the trapped and equilibrium vacancy concentrations, respectively, τ is the relaxation time, ω_R and ω_T are the vacancy release and trapping rates, respectively, and χ is a step function which is 1 in the GB and MI and 0 otherwise. The spatial parameter D_v, required to calculate the diffusion coefficient in (1) and (3), is shown in Fig. 7, while χ is shown in Fig. 8.

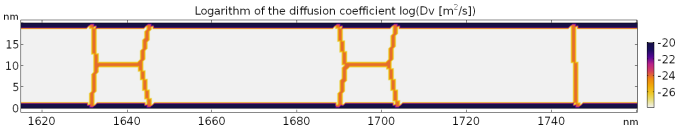

Fig. 7. Microstructure dependent vacancy diffusion coefficient D_v, used for the EM simulation in (3).

Solving (4) gives the time dependent change in the vacancy concentration inside the copper film. The rise of vacancies at one end of the wire and hillocks on the other end results in the rise in tensile and compressive stresses, respectively. Once

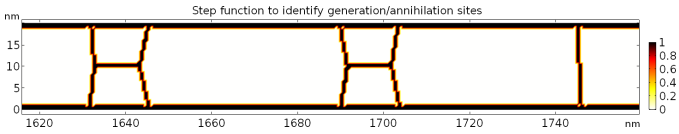

Fig. 8. Step function used to make sure vacancy generation and annihilation are only modeled in the GB and MI.

a critical stress level is reached, the material can no longer conduct current, resulting in failure.

IV. Simulation Results

The first set of simulations were carried out using bulk copper parameters and without including any microstructure components. The simulations were performed on a wire with a height of 20nm with varying lengths of 250nm, 500nm, 1000nm, and 2000nm, with the results shown in Fig. 9. While the slope of the increasing vacancy concentration is the same at all lengths, we note that the line reaches a steady state sooner, due to the atom back flux affecting the vacancy concentration. The effect of the back flux is also noted in the reduction in the vacancy concentration after about 10^5 seconds for the 2000nm long line. This occurs because atoms concentrating at one end of the wire start to reach peak concentrations and start diffusing more towards the end where the vacancies are forming. The shorter the wire is, the sooner this takes place.

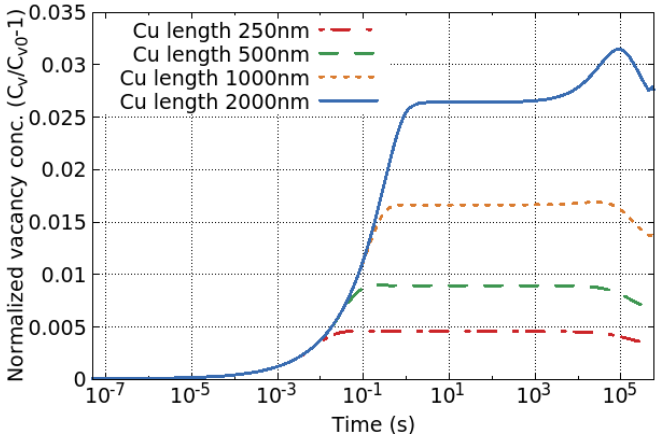

Fig. 9. Vacancy concentration in copper while ignoring microstructure effects for different line lengths with the line thickness set to 20nm.

Sample simulations were performed on a thin copper line using grid and mesh resolutions of 0.4nm, 0.5nm, 1nm, 1.5nm, 2nm, and 2.5nm, with results for the vacancy concentration shown in Fig. 10. A large variation between the bulk and the granular copper structure can be noted, both in an increase in the vacancy concentration and in the early time at with which EM is initiated. We note also how well the 1nm grid resolution replicates the smaller grids. Using a 1nm grid spacing instead of 0.5nm allows for a four-fold decrease in simulation time and memory use, a meaningful advantage of this framework.

In Fig. 11, the EM-induced stress is plotted for various grid and mesh rosolutions. Here we note that when the microstructure is not included and the copper line is treated as a bulk material, the induced stress is overestimated, but

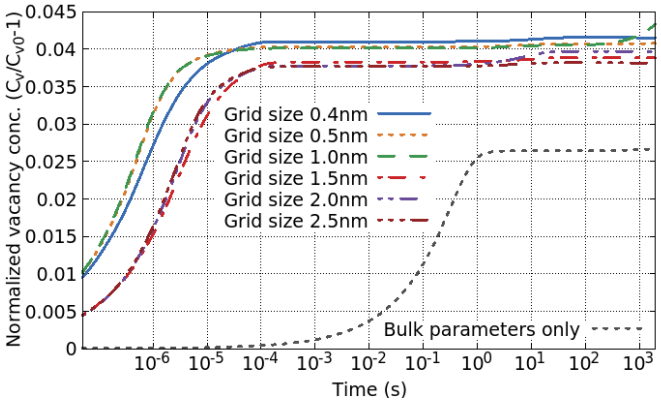

Fig. 10. Vacancy concentration using different mesh resolutions with the GB thickness set to 1nm. The black dotted line represents bulk copper.

not significantly. We also note that grid spacings greater than 0.5nm no longer reproduce the desired results and actually underestimate the induced stress levels.

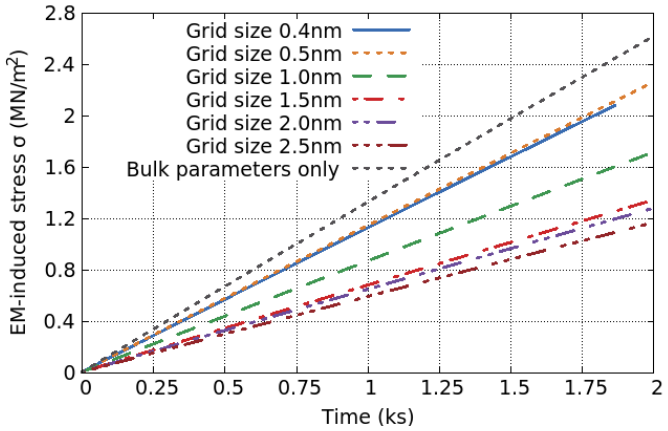

Fig. 11. EM-induced hydrostatic stress using different mesh resolutions with the GB thickness set to 1nm. The black dotted line represents bulk copper.

V. Conclusion

Bulk electromigration models underestimate the time at which electromigration effects are initiated as well as the vacancy concentration level at which back flux begins to take effect. For copper nano-interconnects it is essential to include the grain boundaries and material interfaces in any EM model due to their influence on conductivity and atom diffusivity. Previous attempts have included introducing GBs and MIs as a thin material independent of a copper grain or treating each grain in a copper line as independent. However, both of these methods require very fine and complex meshes. Here we presented a modeling framework which takes into consideration the grain boundaries and material interfaces while minimizing the computational effort and the simulation time. This is achieved by introducing spatial material parameters for the essential aspects of an EM model: atom diffusivity and conductivity. This allows to use coarser meshes, while still achieving reasonable accuracy for the vacancy concentration change during simulation.

ACKNOWLEDGMENT

The research leading to these results has received funding from the European Union's Horizon 2020 research and innovation programme under grant agreement No 688101 SUPERAID7.

REFERENCES

[1] T. Sun, B. Yao, A. P. Warren, K. Barmak, M. F. Toney, R. E. Peale, and K. R. Coffey, "Surface and grain-boundary scattering in nanometric Cu films," *Physical Review B*, vol. 81, no. 15, p. 155454(12), 2010.

[2] A. Mayadas and M. Shatzkes, "Electrical-resistivity model for polycrystalline films: the case of arbitrary reflection at external surfaces," *Physical review B*, vol. 1, no. 4, p. 1382(8), 1970.

[3] K. Fuchs, "The conductivity of thin metallic films according to the electron theory of metals," in *Mathematical Proceedings of the Cambridge Philosophical Society*, vol. 34, no. 1. Cambridge University Press, 1938, pp. 100–108.

[4] P. Mulvaney, "Surface plasmon spectroscopy of nanosized metal particles," *Langmuir*, vol. 12, no. 3, pp. 788–800, 1996.

[5] H. Ceric, R. L. de Orio, J. Cervenka, and S. Selberherr, "A comprehensive TCAD approach for assessing electromigration reliability of modern interconnects," *IEEE Transactions on Device and Materials Reliability*, vol. 9, no. 1, pp. 9–19, 2009.

[6] A. Naeemi and J. D. Meindl, "Carbon nanotube interconnects," *Annual Review of Materials Research*, vol. 39, pp. 255–275, 2009.

[7] B. Uhlig, J. Liang, J. Lee, R. Ramos, A. Dhavamani, N. Nagy, J. Dijon, H. Okuno, D. Kalita, V. Georgiev *et al.*, "Progress on carbon nanotube BEOL interconnects," in *Design, Automation & Test in Europe Conference & Exhibition (DATE)*, 2018, pp. 937–942.

[8] "International Technology Roadmap for Semiconductors," IRC, Tech. Rep., 2015.

[9] R. De Orio, H. Ceric, and S. Selberherr, "Physically based models of electromigration: From Black's equation to modern TCAD models," *Microelectronics Reliability*, vol. 50, no. 6, pp. 775–789, 2010.

[10] L. Filipovic, R. de Orio, W. Zisser, and S. Selberherr, "Modeling electromigration in nanoscaled copper interconnects," in *Simulation of Semiconductor Processes and Devices (SISPAD), 2017 International Conference on*. IEEE, 2017, pp. 161–164.

[11] R. Quey, P. Dawson, and F. Barbe, "Large-scale 3D random polycrystals for the finite element method: Generation, meshing and remeshing," *Computer Methods in Applied Mechanics and Engineering*, vol. 200, no. 17-20, pp. 1729–1745, 2011.

[12] *COMSOL Multiphysics, Version: 5.0*, 2014.

[13] X. Zhu, G. Zhang, and C. Yan, "Grain boundary effects on microstructural stability of nanocrystalline metallic materials," in *Study of Grain Boundary Character*, T. Tanski, Ed. InTechOpen, 2017, ch. 7.

[14] J. S. Clarke, C. George, C. Jezewski, A. M. Caro, D. Michalak, and J. Torres, "Process technology scaling in an increasingly interconnect dominated world," in *Symposium on VLSI Technology (VLSI-Technology): Digest of Technical Papers*. IEEE, 2014, pp. 1–2.